WO9822441-A2 and WO9822494-A2 filed by Athena Neurosciences and Eli Lilly. The identity of each compound was confirmed by ^{1}H-NMR and mass spectrometry.

Received 7 January; accepted 11 February 2002.

1. Selkoe, D. J. Alzheimer's disease: genes, proteins and therapies. *Physiol. Rev.* **81,** 742–761 (2001).
2. Pike, C. J. Walencewicz, A. J., Glabe, C. G. & Cotman, C. W. *In vitro* aging of β-amyloid protein causes peptide aggregation and neurotoxicity. *Brain Res.* **563,** 311–314 (1991).
3. Lorenzo, A. & Yankner, B. A. β-amyloid neurotoxicity requires fibril formation and is inhibited by congo red. *Proc. Natl Acad. Sci. USA* **91,** 12243–12247 (1994).
4. Terry, R. D. *et al.* Physical basis of cognitive alterations in Alzheimer's disease: synapse loss is the major correlate of cognitive impairment. *Ann. Neurol.* **30,** 572–580 (1991).
5. Dickson, D. W. *et al.* Correlations of synaptic and pathological markers with cognition of the elderly. *Neurobiol. Aging* **16,** 285–298 (1995).
6. Lue, L. F. *et al.* Soluble amyloid β peptide concentration as a predictor of synaptic change in Alzheimer's disease. *Am. J. Pathol.* **155,** 853–862 (1999).
7. McLean, C. A. *et al.* Soluble pool of Aβ amyloid as a determinant of severity of neurodegeneration in Alzheimer's disease. *Ann. Neurol.* **46,** 860–866 (1999).
8. Podlisny, M. B. *et al.* Aggregation of secreted amyloid β-protein into sodium dodecyl sulfate-stable oligomers in cell culture. *J. Biol. Chem.* **270,** 9564–9570 (1995).
9. Morishima-Kawashima, M. & Ihara, Y. The presence of amyloid β-protein in the detergent-insoluble membrane compartment of human neuroblastoma cells. *Biochemistry* **37,** 15247–15253 (1998).
10. Walsh, D. M., Tseng, B. P., Rydel, R. E., Podlisny, M. B. & Selkoe, D. J. Detection of intracellular oligomers of amyloid β-protein in cells derived from human brain. *Biochemistry* **39,** 10831–10839 (2000).
11. Xia, W. M. *et al.* Enhanced production and oligomerization of the 42-residue amyloid β-protein by Chinese hamster ovary cells stably expressing mutant presenilins. *J. Biol. Chem.* **272,** 7977–7982 (1997).
12. Hsia, A. Y. *et al.* Plaque-independent disruption of neural circuits in Alzheimer's disease mouse model. *Proc. Natl Acad. Sci. USA* **96,** 3228–3233 (1999).
13. Mucke, L. *et al.* High-level neuronal expression of Aβ1-42 in wild-type human amyloid protein precursor transgenic mice: synaptotoxicity without plaque formation. *J. Neurosci.* **20,** 4050–4058 (2000).
14. Hartley, D. M. *et al.* Protofibrillar intermediates of amyloid β-protein induce acute electrophysiological changes and progressive neurotoxicity in cortical neurons. *J. Neurosci.* **19,** 8876–8884 (1999).
15. Xia, W. *et al.* Presenilin complexes with the C-terminal fragments of amyloid precursor protein at the sites of amyloid β-protein generation. *Proc. Natl Acad. Sci. USA* **97,** 9299–9304 (2000).
16. Kim, J. H., Anwyl, R., Suh, Y. H., Djamgoz, M. B. & Rowan, M. J. Use-dependent effects of amyloidogenic fragments of β-amyloid precursor protein on synaptic plasticity in rat hippocampus *in vivo*. *J. Neurosci.* **21,** 1327–1333 (2001).
17. Qiu, W. Q. *et al.* Insulin-degrading enzyme regulates extracellular levels of amyloid β-protein by degradation. *J. Biol. Chem.* **273,** 32730–32738 (1998).
18. Lambert, M. P. *et al.* Diffusible, nonfibrillar ligands derived from $A\beta_{1-42}$ are potent central nervous system neurotoxins. *Proc. Natl Acad. Sci. USA* **95,** 6448–6453 (1998).
19. Walsh, D. M. *et al.* Amyloid β-protein fibrillogenesis: structure and biological activity of protofibrillar intermediates. *J. Biol. Chem.* **274,** 25945–25952 (1999).
20. Chui, D.-H. *et al.* Transgenic mice with Alzheimer presenilin 1 mutations show accelerated neurodegeneration without amyloid plaque formation. *Nature Med.* **5,** 560–564 (1999).
21. Chen, G. *et al.* A learning deficit related to age and β-amyloid plaques in a mouse model of Alzheimer's disease. *Nature* **408,** 975–979 (2000).
22. Lewis, J. *et al.* Enhanced neurofibrillary degeneration in transgenic mice expressing mutant tau and APP. *Science* **293,** 1487–1491 (2001).
23. Larson, J., Lynch, G., Games, D. & Seubert, P. Alterations in synaptic transmission and long-term potentiation in hippocampal slices for young and aged PDAPP mice. *Brain Res.* **840,** 23–35 (1999).
24. Moechars, D. *et al.* Early phenotypic changes in transgenic mice that overexpress different mutants of amyloid precursor protein in brain. *J. Biol. Chem.* **274,** 6483–6492 (1999).
25. Chapman, P. F. *et al.* Impaired synaptic plasticity and learning in aged amyloid precursor protein transgenic mice. *Nature Neurosci.* **2,** 271–276 (1999).
26. Fitzhohn, S. M. *et al.* Age-related impairment of synaptic transmission but normal long-term potentiation in transgenic mice that overexpress the human APP695SWE mutant form of amyloid precursor protein. *J. Neurosci.* **21,** 4691–4698 (2001).
27. Rochet, J. C. & Lansbury, P. T.Jr Amyloid fibrillogenesis: themes and variations. *Curr. Opin. Struct. Biol.* **10,** 60–68 (2000).
28. Chiti, F. *et al.* Designing conditions for *in vitro* formation of amyloid protofilaments and fibrils. *Proc. Natl Acad. Sci. USA* **96,** 3590–3590 (1999).
29. Chesneau, V. & Rosner, M. R. Functional human insulin-degrading enzyme can be expressed in bacteria. *Protein Expr. Purif.* **19,** 91–98 (2000).
30. Getman, D. P. *et al.* Discovery of a novel class of potent HIV-1 protease inhibitors containing the (R)-(hydroxyethyl)urea isostere. *J. Med. Chem.* **36,** 288–291 (1993).

Acknowledgements

We thank M. Rosner and V. Chesneau for the gift of the pProExH6HA IDE expression vector, B. Zheng for ELISA analysis, S. Mansourian for assistance in the preparation of illustrations and W. T. Kimberly, W. P. Esler and D. M. Hartley for discussions. Supported by NIH grants (to D.J.S. and M.S.W.) and by Enterprise Ireland and the Health Research Board Ireland (M.R. and R.A.).

Competing interests statement

The authors declare that they have no competing financial interests.

Correspondence and requests for materials should be addressed to D.J.S. (e-mail: dselkoe@rics.bwh.harvard.edu).

A global disorder of imprinting in the human female germ line

Hannah Judson, Bruce E. Hayward, Eamonn Sheridan & David T. Bonthron

University of Leeds, Molecular Medicine Unit, St. James's University Hospital, Leeds LS9 7TF, UK

Imprinted genes are expressed differently depending on whether they are carried by a chromosome of maternal or paternal origin. Correct imprinting is established by germline-specific modifications; failure of this process underlies several inherited human syndromes[1–5]. All these imprinting control defects are *cis*-acting, disrupting establishment or maintenance of allele-specific epigenetic modifications across one contiguous segment of the genome. In contrast, we report here an inherited global imprinting defect. This recessive maternal-effect mutation disrupts the specification of imprints at multiple, non-contiguous loci, with the result that genes normally carrying a maternal methylation imprint assume a paternal epigenetic pattern on the maternal allele. The resulting conception is phenotypically indistinguishable from an androgenetic complete hydatidiform mole[6], in which abnormal extra-embryonic tissue proliferates while development of the embryo is absent or nearly so. This disorder offers a genetic route to the identification of *trans*-acting oocyte factors that mediate maternal imprint establishment.

Although normally sporadic, complete hydatidiform mole (CHM) is occasionally familial, with affected women repeatedly having pregnancies of this type. These repetitive CHMs are not androgenetic but biparental (BiCHM)[7–9]. By analogy to disorders like Prader–Willi syndrome (which can result from sporadic uniparental disomy or from familial imprinting control mutations), we considered that BiCHM might arise from a global inherited failure of maternal imprinting.

We studied the sixth molar pregnancy of the index case in a BiCHM family with complex consanguinity, originating from the Mirpur region of Pakistan. We demonstrated biparental origin of the BiCHM DNA using markers on six autosomes.

Imprinted genes are associated with differentially methylated regions (DMRs), either 'primary' (established during gametogenesis) or 'secondary' (established later in embryogenesis). We used bisulphite sequencing[10] to compare methylation in the BiCHM and suitable controls, including uniparental DNAs and first-trimester chorionic villus samples, which like CHMs, are of trophoblastic origin.

The Beckwith–Wiedemann region of 11p15 contains two putative primary imprint control regions, at *H19* and *KCNQ1OT1*, ~500 kilobases (500 kb) apart. The DMR ~2-kb upstream of *H19* normally shows paternal-specific germline methylation[11], and is therefore an important control locus (Fig. 1a). Parthenogenetic (Pg) and androgenetic (Ag) control DNAs were respectively completely unmethylated and completely methylated at all CpG dinucleotides, as expected. The BiCHM DNA shows a differentially methylated pattern, like that of normal controls. Cloned polymerase chain reaction (PCR) products from BiCHM were either almost completely methylated or completely unmethylated, as expected for paternal or maternal alleles, respectively.) This maintenance of normal *H19* differential methylation in the BiCHM is as predicted, if only imprinting in the female germ line is affected.

At loci with a maternal methylation imprint (Fig. 1b–e), a very different pattern is seen. The *KCNQ1OT1* primary DMR[12,13] becomes methylated during oogenesis[14]. As expected, our normal control DNAs are uniformly haplo-methylated (C and T bands of similar intensity at each original CpG position), and the partheno-

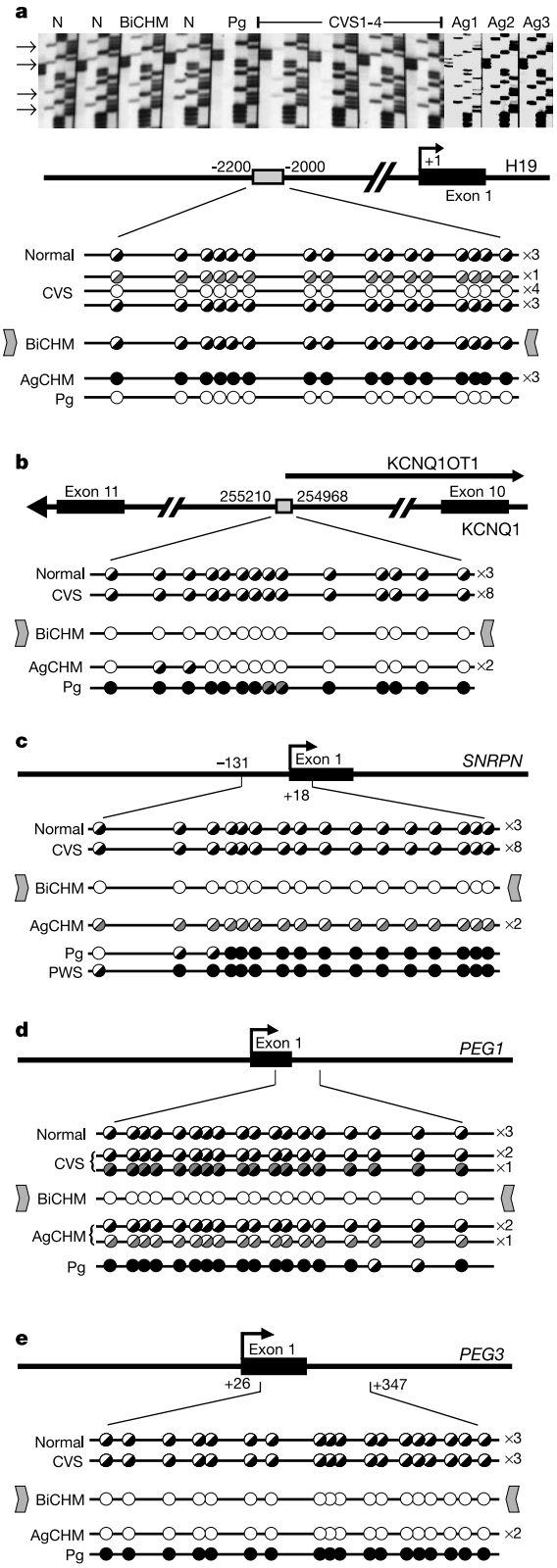

Figure 1 Bisulphite sequencing of DMRs in imprinted genes. Circles represent positions and methylation of individual CpGs, as follows: filled, methylated; open, unmethylated; half-filled black/white, haplo-methylated; black/grey, predominantly methylated; grey/white, predominantly unmethylated. Identical results from multiple controls are collated, numbers indicated to the right. **a**, *H19*. The first and last CpG are numbered relative to the transcriptional start site. Arrows indicate differentially methylated C residues on the gel. N, adult control DNA. Lanes: ACGT, left to right. **b**, *KCNQ1OT1*. Numbering refers to accession AJ006345. **c**, *SNRPN*. Numbering relates to the first nucleotide of exon 1. PWS, Prader–Willi syndrome. **d**, *PEG1*. **e**, *ZIM2/PEG3*. CVS, chorionic villus sample.

genetic sample fully methylated. In contrast, the BiCHM DNA is completely unmethylated, its maternal *KCNQ1OT1* allele thus having a paternal epigenotype.

The 5′ DMR of *SNRPN* (15q) behaved similarly. In the mouse, this is a primary imprint[15], but in humans may only become established in early post-zygotic development[16]. In the BiCHM, this DMR was completely unmethylated (paternal epigenotype), whereas the parthenogenetic and Prader–Willi controls had the opposite epigenotype (almost all CpGs completely methylated). Chorionic villus samples and other normal controls were uniformly haplo-methylated (Fig. 1c). AgCHM were hypomethylated compared to normal DNA, but unlike the BiCHM did show faint bands indicating some (presumably secondary) CpG methylation (see also Supplementary Information).

PEG1 (7q32) and *ZIM2/PEG3* (19q13.4)[17,18] both have maternally methylated DMRs. It is not known if these are primary imprints, although the demethylated paternal *PEG1* epigenotype is established during spermatogenesis[11]. In the BiCHM, these DMRs are both completely unmethylated (paternal epigenotype on both alleles). At *ZIM2/PEG3*, the controls appear as predicted, the normal DNAs being haplo-methylated, the PgDNA completely methylated, and the AgCHM, like the BiCHM, unmethylated (Fig. 1e). However, at *PEG1*, whilst the normal and parthenogenetic samples are respectively haplo-methylated and completely methylated (as expected) the AgCHM DNAs show a variable degree of incomplete methylation (Fig. 1d).

To test whether the BiCHM methylation abnormalities truly reflect a defect of maternal gametic imprinting, rather than being secondary to the molar phenotype, we examined a complex locus, *GNAS1*, that has multiple imprinted transcripts and at least three separate DMRs[19–22] (Fig. 2). In murine *Gnas*, the exon 1A DMR is a primary imprint, whereas the upstream DMRs only become established during the blastocyst stage[22]. Likewise, *GNAS1* imprinting mutations that cause type Ib pseudohypoparathyroidism (PHP-Ib) always alter exon 1A methylation, with the other DMRs only sometimes affected[5]. Therefore, a maternal germline imprinting defect should involve failure to methylate the maternal allele of exon 1A. The maternal NESP55, XLαs, and antisense promoter DMRs (all 35–50 kb upstream) should then secondarily assume a paternal epigenotype, becoming respectively methylated, unmethylated, and unmethylated. This prediction was almost completely fulfilled. At exon 1A, the parthenogenetic control, as expected, is completely methylated, whereas the BiCHM is completely unmethylated, indicating failure to establish the maternal primary imprint. There is some variability in methylation in control samples; two of ten chorionic villus sample DNAs are hypomethylated, and one of three AgCHM appears partially methylated, suggesting that some secondary methylation must have appeared at this locus. Nonetheless, the unmethylated status of the BiCHM is as predicted, and that this represents a true germline defect is supported by analysis of the other DMRs at this locus.

The NESP55 DMR becomes methylated on the paternal allele in the blastocyst stage, possibly secondary to antisense transcription[21,22]. BiCHM and AgCHM are both completely methylated at this DMR (paternal epigenotype on both alleles). All other controls show the expected methylation patterns. Thus, the postzygotic mechanism that sets up the secondary paternal NESP55 imprint remains operative in the BiCHM, but in the absence of a maternal gametic imprint at 1A this yields a paternal methylation pattern on both, rather than one, NESP55 alleles.

We also examined two regions ~3 kb apart, within a large (5-kb) CpG island spanning the antisense promoter and XLαs exon. At the antisense DMR, the BiCHM again shows a paternal epigenotype (this time unmethylated) on both alleles. This lack of methylation is distinctive, even though both AgCHMs show a minor degree of secondary methylation at this locus.

The maternal XLαs allele becomes methylated during the blas-

tocyst stage[22]. Here we initially saw no sign of abnormal methylation in the BiCHM, the DNA appearing haplo-methylated. Similar partial methylation at this DMR, independent of correct maternal methylation at exon 1A, has been seen with *cis*-acting *GNAS1* imprinting defects that cause PHP-Ib; several such families have an abnormal (paternal) methylation pattern at exon 1A and NESP55, whereas the XLαs DMR appears unaffected[5]. Cloning of the BiCHM bisulphite-PCR products, however, revealed a disordered pattern of partial methylation scattered irregularly across the clones, rather than the normal grouping into completely methylated and completely unmethylated clones (see Supplementary Information). A similar analysis has not been reported for the PHP-Ib mutations. Thus, despite the appearance of some methylation at the XLαs DMR, the overall evidence from the four DMRs argues compellingly for a *GNAS1* imprinting defect in BiCHM, very similar to that resulting from some maternally transmitted *cis*-acting imprinting mutations.

The contrasting behaviour of *H19* and *GNAS1*-NESP55 in the BiCHM is noteworthy. Although both DMRs are normally paternally methylated, for *H19* this is primary, and therefore unaffected by an oocyte defect. At NESP55, paternal methylation is secondary to lack of a maternal imprint at 1A, and hence occurs on both alleles in the BiCHM. This difference suggests that the BiCHM defect is not a generalized failure of methylation maintenance, but reflects specific events in the female germ line. Also consistent with this conclusion was the observation of a normal methylated status in the BiCHM at eight CpGs in an intragenic (non-CpG island) region of the non-imprinted *KHK* gene (not shown). Other evidence argues that the BiCHM methylation abnormalities reflect a specific imprinting defect, rather than changes peculiar to trophoblast derivatives. First, we see neither random nor generalized hypo- or hyper-methylation; instead, at each DMR, the direction of the BiCHM methylation abnormality is specifically as predicted for a maternal germline defect. Second, despite some minor inter-sample variation, chorionic villus sample DNAs (which, like the CHMs, are first trimester trophoblast derivatives) typically had normal differential methylation, and never had a 'paternal-only' epigenotype resembling that of the AgCHM and BiCHM.

Cis-acting mutations that disrupt imprinting at individual loci[1–5,12,13,23–24] show sex-dependent dominant (vertical) transmission. In contrast, BiCHM is a pure maternal-effect defect; affected women may have molar pregnancies with different partners[9], but are otherwise healthy. Its presumed autosomal recessive inheritance pattern implies a *trans*-acting molecular defect, consistent with the involvement of multiple dispersed imprinted loci. Of all imprinted loci examined, only *H19* (as predicted) showed a normal differentially methylated pattern in the BiCHM. Because most gametic imprints are imposed in the female rather than the male germ line[25], the great majority of all imprinted loci are probably affected by this genetic defect. A recessive *Dnmt3L* mutation, although also conferring male sterility, prevents specification of maternal imprints in the mouse germ line[26]. In the family studied here, lack of homozygosity for the corresponding human locus, as well as for a previously suggested 19q BiCHM locus[7](see

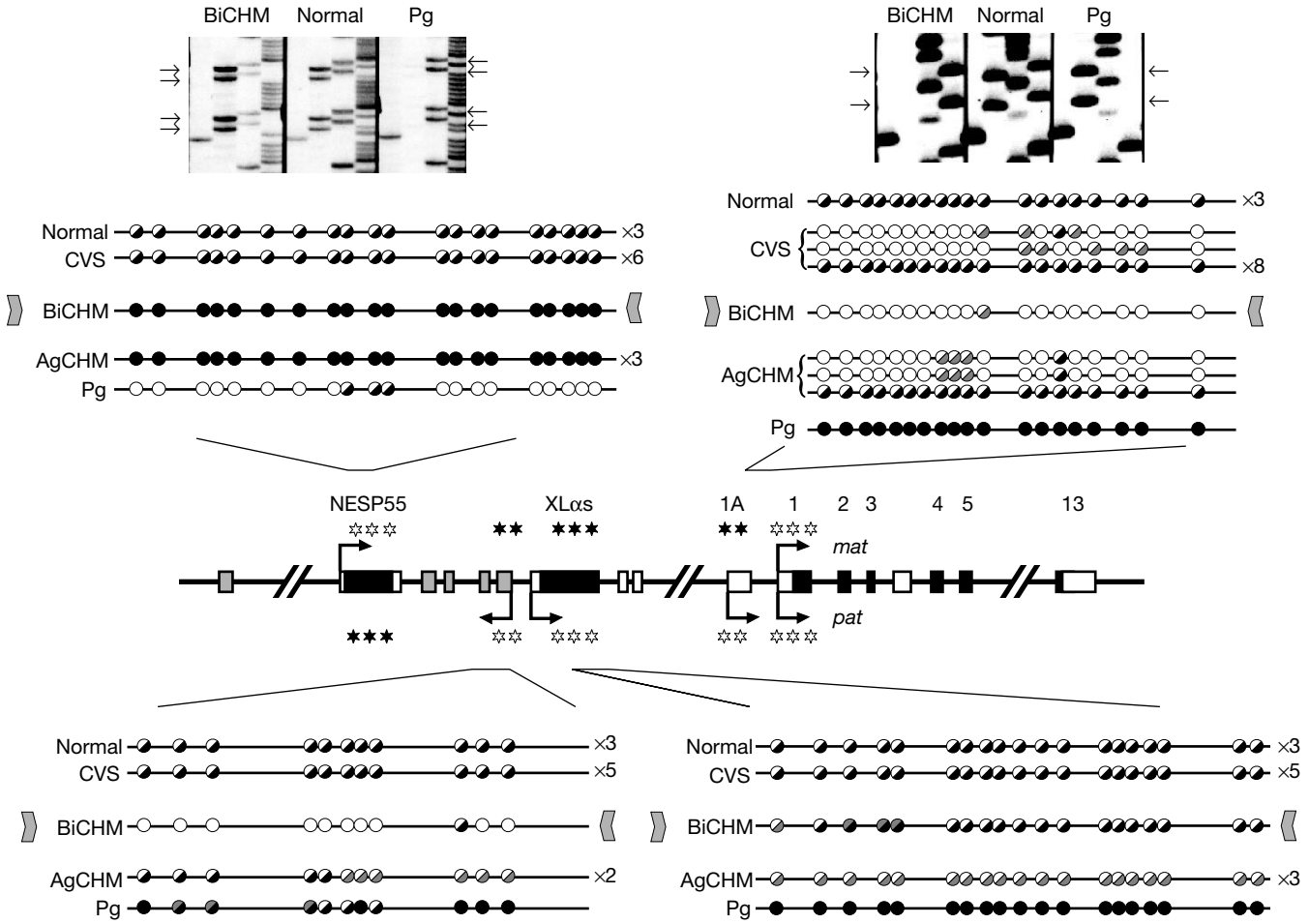

Figure 2 Bisulphite analysis of *GNAS1*. At the top, the contrasting methylation status at the 1A and *NESP55* DMRs is illustrated; arrows on the gels indicate differentially methylated residues. The remainder of the figure summarizes data for the whole locus (for symbols see Fig. 1). In the schematic map of *GNAS1*, coding regions are black, antisense exons grey. All alternative first exons on the sense strand splice onto exon 2 (refs 5, 21). Arrows above and below the line indicate maternal and paternal transcription, respectively. Normally methylated or unmethylated status of CpG islands is shown by filled or open stars, respectively.

Supplementary Information) makes involvement of either of these loci unlikely. However, the BiCHM defect should eventually be identifiable through autozygosity mapping. □

Methods

Detailed methods are available in Supplementary Information.

DNA samples

BiCHM DNA was extracted from a short-term culture of the evacuation products from the sixth pregnancy of the index case. Four of her first five conceptions had previously been histologically confirmed as CHM, and demonstrated to be biparental using archival pathological material. Parthenogenetic DNA was previously described[27]. Adult control blood DNAs were from the index case, her husband, and an unrelated individual. Fluorescent PCR analysis of markers D1S2691, D5S495, D10S189, D13S1293, D17S946, D19S210 and D19S413 was performed by standard methods on DNA from the cultured BiCHM and from the index case and her husband; all these markers were fully informative for demonstrating both maternal and paternal allelic contributions to the mole.

Bisulphite-PCR analysis of DNA methylation

The protocol was adapted from previously described methods[10,24]. Briefly, genomic DNA was denatured and bisulphite-treated to convert unmethylated cytosines to thymines. PCR products encompassing the DMRs of each imprinted locus were then generated. Only one strand was amplified at each locus. Products were analysed by direct sequencing, because at some loci the two modified alleles clone with different efficiencies. Cloning was therefore used only to assess the allelic separation of C and T at haplo-methylated loci (see text).

Received 18 September 2001; accepted 21 January 2002.

1. Sutcliffe, J. S. *et al.* Deletions of a differentially methylated CpG island at the SNRPN gene define a putative imprinting control region. *Nature Genet.* **8,** 52–58 (1994).
2. Buiting, K. *et al.* Inherited microdeletions in the Angelman and Prader-Willi syndromes define an imprinting centre on human chromosome 15. *Nature Genet.* **9,** 395–400 (1995).
3. Reik, W. *et al.* Imprinting mutations in the Beckwith-Wiedemann syndrome suggested by altered imprinting pattern in the IGF2-H19 domain. *Hum. Mol. Genet.* **4,** 2379–2385 (1995).
4. Gardner, R. J. *et al.* An imprinted locus associated with transient neonatal diabetes mellitus. *Hum. Mol. Genet.* **9,** 589–596 (2000).
5. Liu, J. *et al.* A GNAS1 imprinting defect in pseudohypoparathyroidism type IB. *J. Clin. Invest.* **106,** 1167–1174 (2000).
6. Kajii, T. & Ohama, K. Androgenetic origin of hydatidiform mole. *Nature* **268,** 633–634 (1977).
7. Moglabey, Y. B. *et al.* Genetic mapping of a maternal locus responsible for familial hydatidiform moles. *Hum. Mol. Genet.* **8,** 667–671 (1999).
8. Helwani, M. N. *et al.* A familial case of recurrent hydatidiform molar pregnancies with biparental genomic contribution. *Hum. Genet.* **105,** 112–115 (1999).
9. Fisher, R. A., Khatoon, R., Paradinas, F. J., Roberts, A. P. & Newlands, E. S. Repetitive complete hydatidiform mole can be biparental in origin and either male or female. *Hum. Reprod.* **15,** 594–598 (2000).
10. Clark, S. J., Harrison, J., Paul, C. L. & Frommer, M. High sensitivity mapping of methylated cytosines. *Nucleic Acids Res.* **22,** 2990–2997 (1994).
11. Kerjean, A. *et al.* Establishment of the paternal methylation imprint of the human H19 and MEST/PEG1 genes during spermatogenesis. *Hum. Mol. Genet.* **9,** 2183–2187 (2000).
12. Lee, M. P. *et al.* Loss of imprinting of a paternally expressed transcript, with antisense orientation to KVLQT1, occurs frequently in Beckwith-Wiedemann syndrome and is independent of insulin-like growth factor II imprinting. *Proc. Natl Acad. Sci. USA* **96,** 5203–5208 (1999).
13. Ohta, T. *et al.* Imprinting-mutation mechanisms in Prader-Willi syndrome. *Am. J. Hum. Genet.* **64,** 397–413 (1999).
14. Engemann, S. *et al.* Sequence and functional comparison in the Beckwith-Wiedemann region: implications for a novel imprinting centre and extended imprinting. *Hum. Mol. Genet.* **9,** 2691–2706 (2000).
15. Shemer, R., Birger, Y., Riggs, A. D. & Razin, A. Structure of the imprinted mouse Snrpn gene and establishment of its parental-specific methylation pattern. *Proc. Natl Acad. Sci. USA* **94,** 10267–10272 (1997).
16. El-Maarri, O. *et al.* Maternal methylation imprints on human chromosome 15 are established during or after fertilization. *Nature Genet.* **27,** 341–344 (2001).
17. Kaneko-Ishino, T. *et al.* Peg1/Mest imprinted gene on chromosome 6 identified by cDNA subtraction hybridization. *Nature Genet.* **11,** 52–59 (1995).
18. Murphy, S. K., Wylie, A. A. & Jirtle, R. L. Imprinting of PEG3, the human homologue of a mouse gene involved in nurturing behavior. *Genomics* **71,** 110–117 (2001).
19. Hayward, B. E. *et al.* The human GNAS1 gene is imprinted and encodes distinct paternally and biallelically expressed G proteins. *Proc. Natl Acad. Sci. USA* **95,** 10038–10043 (1998).
20. Hayward, B. E., Moran, V., Strain, L. & Bonthron, D. T. Bidirectional imprinting of a single gene: GNAS1 encodes maternally, paternally, and biallelically derived proteins. *Proc. Natl Acad. Sci. USA* **95,** 15475–15480 (1998).
21. Hayward, B. E. & Bonthron, D. T. An imprinted antisense transcript at the human GNAS1 locus. *Hum. Mol. Genet.* **9,** 835–841 (2000).
22. Liu, J., Yu, S., Litman, D., Chen, W. & Weinstein, L. S. Identification of a methylation imprint mark within the mouse Gnas locus. *Mol. Cell Biol.* **20,** 5808–5817 (2000).
23. Smilinich, N. J. *et al.* A maternally methylated CpG island in KvLQT1 is associated with an antisense paternal transcript and loss of imprinting in Beckwith-Wiedemann syndrome. *Proc. Natl Acad. Sci. USA* **96,** 8064–8069 (1999).
24. Kamiya, M. *et al.* The cell cycle control gene ZAC/PLAGL1 is imprinted—a strong candidate gene for transient neonatal diabetes. *Hum. Mol. Genet.* **9,** 453–460 (2000).
25. Reik, W. & Walter, J. Evolution of imprinting mechanisms: the battle of the sexes begins in the zygote. *Nature Genet.* **27,** 255–256 (2001).
26. Bourc'his, D., Xu, G.-L., Lin, C.-S., Bollman, B. & Bestor, T. H. Dnmt3L and the establishment of maternal genomic imprints. *Science* **294,** 2536–2539 (2001); advance online publication, 29 November 2001 (DOI 10,1126/Science.1065848).
27. Strain, L., Warner, J. P., Johnston, T. & Bonthron, D. T. A human parthenogenetic chimaera. *Nature Genet.* **11,** 164–169 (1995).

Supplementary Information accompanies the paper on *Nature's* website (http://www.nature.com).

Acknowledgements

We thank R. Fisher for supplying androgenetic CHM DNAs, and G. Taylor for Prader–Willi and chorionic villus sample DNA samples. This work was supported by the Wellcome Trust.

Competing interests statement

The authors declare that they have no competing financial interests.

Correspondence and requests for materials should be addressed to D.T.B. (e-mail: d.t.bonthron@leeds.ac.uk).

Bone marrow cells adopt the phenotype of other cells by spontaneous cell fusion

Naohiro Terada*†, Takashi Hamazaki*, Masahiro Oka*, Masanori Hoki*, Diana M. Mastalerz*, Yuka Nakano‡, Edwin M. Meyer‡, Laurence Morel*, Bryon E. Petersen*† & Edward W. Scott†§

** Department of Pathology, † Program in Stem Cell Biology, Shands Cancer Center, ‡ Department of Pharmacology, § Department of Molecular Genetics and Microbiology, University of Florida College of Medicine, Gainesville, Florida 32610, USA*

Recent studies have demonstrated that transplanted bone marrow cells can turn into unexpected lineages including myocytes, hepatocytes, neurons and many others[1]. A potential problem, however, is that reports discussing such 'transdifferentiation' *in vivo* tend to conclude donor origin of transdifferentiated cells on the basis of the existence of donor-specific genes such as Y-chromosome markers[1]. Here we demonstrate that mouse bone marrow cells can fuse spontaneously with embryonic stem cells in culture *in vitro* that contains interleukin-3. Moreover, spontaneously fused bone marrow cells can subsequently adopt the phenotype of the recipient cells, which, without detailed genetic analysis, might be interpreted as 'dedifferentiation' or transdifferentiation.

Recent progress in stem cell research indicates that certain mammalian cells, even from adults, maintain a high degree of plasticity for multilineage cell differentiation. The transferred nuclei from adult cells could be reprogrammed by a factor or factors in the cytoplasm of oocytes, showing the same potential for normal animal development as early embryonic nuclei[2]. More recently, neural stem cells were demonstrated to differentiate into virtually every cell type when they were injected into blastocysts *in vivo* or cultured *in vitro* with differentiating embryonic stem cells[3]. This indicated that the extracellular factor(s) of blastocysts or embryonic stem cells, or cell–cell interaction of neural stem cells with such embryonic cells, might be sufficient for reprogramming adult cells into a more pluripotent status. To this end, we attempted to establish a culture of pluripotent stem cells *in vitro* from adult cells (bone marrow cells) by nurturing them with embryonic stem cells. Bone marrow contains haematopoietic stem cells producing

Supplementary information for Judson H. *et al.* "A global disorder of imprinting in the human female germline."

Detailed methods

Methylation analysis of differentially methylated regions (DMRs) of imprinted genes

DNA (1 µg / 50 µl) was digested overnight with 25 units of *Pvu*II (or *Bam*HI in the case of *SNRPN*, where a *Pvu*II site lies between the primers). Ethanol-precipitated products were resuspended in 50 µl TE buffer (pH 8.0). Following denaturation (with 5.5 µl 3M NaOH at 37°C for 15 minutes), 30 µl 10 mM hydroquinone, and 520 µl (3.6M) sodium bisulphite pH 5.0 were added. The reactions were incubated at 55°C for 16 hours. DNA was purified with Geneclean™ (Bio101), and eluted into 20 µl water. A further denaturation was performed by adding 2.2 µl 3M NaOH and incubating at 37°C for 15 minutes. The denatured modified DNA was ethanol-precipitated and resuspended in 15 µl TE; 2 µl was used per 50 µl PCR reaction. PCR primer sequences and cycling conditions were as follows:

H19: dTGTATAGTATATGGGTATTTTTGGAGGTTT and dTCCTATAAATATCCTATTCCCAAATAACC (Kerjean et al., ref. 11 in main text). 35 cycles of 94, 52, 72ºC; 45, 45, 90 s. Sequencing primer dTTTTGGTTTTATTGTTTGGATGGTA. The region sequenced was nt 6115-6326 of AF087017.

KCNQ1OT1 (LIT1): dTGTTGAGGAGTTTYGGGGAGGATTA and dCACCTCACACCCAACCAATACCTCAT (40 cycles of 94, 50, 72ºC; 45, 45, 60 s). Sequenced with dTTGGTAGGATTTTGTTGAGGAGTTTT or dAAACCAAACTCTTTCAACCAATAAC.

SNRPN: Nested PCR[1]. First round: dGGTTTTTTTTTATTGTAATAGTGTTGTGGGG and dCTCCAAAACAAAAAACTTTAAAACCCAAATTC. Second round: dCAATACTCCAAATCCTAAAAACTTAAAATATC and dGGTTTTAGGGGTTTAGTAGTTTTTTTTTTTTGG (also used as a sequencing primer). 35 cycles of 94, 51, 72ºC; 60, 60, 60 s. 2.5 µl were then diluted into a fresh 50 µl reaction and reamplified for a further 25 cycles.

PEG1: dtygttgttggttagttttgtayggtt and dAAAAATAACACCCCCTCCTCAAAT (Kerjean et al., ref. 11 in main text). 40 cycles of 94, 61, 72ºC; 45, 45, 60s. Sequencing primer dAAAATTTCRACCCAAAAACAACCCC.

ZIM2/PEG3: dAAAAGGTATTAATTATTTATAGTTTGGT and dAAAAATATCCACCCTAAACTAATAA (also used as a sequencing primer). 6 cycles of 94ºC 30s, -1ºC/s ramp to 60ºC, 60ºC 20s (-1ºC/cycle), 72ºC 60s; 6 cycles of 94ºC 30s, -1ºC/s ramp to 55ºC, 55ºC 20s (-1ºC/cycle), 72ºC 60s; 32 cycles of 94ºC 30s, 1ºC/s ramp to 50ºC, 50ºC 20s, 72ºC 60s.

GNAS1. The positions of each amplicon were: exon 1A, nt 29821-30039 of AL121917; NESP55,

106677-107019 of AL132655; XLαs, 120557-120954 of AL132655; antisense promoter, 117154-117607 of AL132655.

GNAS1-1A*:* Nested PCR. First round (35 cycles of 94, 55, 72ºC; 45, 45, 90 s): dTTTTGTTTTTTTTTYGTTTGTTTAT and dACAACTTCRACAACCACCTCRACAAC. Second round (25 cycles using 2 µl of first round products): dTAAACTTCATAACCATCTTCAACATAA and dTTAATTTTTAGGTAGTTAGTTTAGTAGTT (also used as a sequencing primer).

GNAS1-NESP55*:* dTTTTTGTAGAGTTAGAGGGTAGGT (also used as a sequencing primer), and dAAATAAAACAACTCAAAATCTACC (40 cycles of 94, 50, 72ºC; 45, 45, 60 s).

GNAS1-antisense*:* dTATTTGTGTAGGTTTAGTATTTTTGG and dCATCCTCTAAATAACCCAACTAAATC (40 cycles of 94, 54, 72ºC; 45, 45, 60 s). Sequencing primer: dAAACAAAAATCATACCAATCAAAAC.

GNAS1-XLαs*:* dGTTGGTTTTAGAGGAGGTTATAGTT and dCCTCCTCAACTAAAAATCTCTCTAC (40 cycles of 94, 54, 72ºC; 45, 45, 60 s). Sequencing primer: dGTTATTTGAGTTTGATGGAGAAGG.

KHK: dTTTAGTAGTTTTGTTTTGGATGATT and dACAACTAACAAAACACAAACAATTA (8 cycles of 94ºC 30s, 0.5ºC/s ramp to 59ºC, 59ºC [-1ºC/cycle] 30s, 72ºC 60s; 32 cycles of 94ºC 30s, 0.5ºC/s ramp to 50ºC, 50ºC 30s, 72ºC 60s).

PCR products were treated with shrimp alkaline phosphatase and exonuclease I, and cycle-sequenced with a Thermosequenase ^{33}P-labelled terminator kit (AmershamPharmacia). dITP was needed to reduce the effect of GC compressions, which otherwise cause differential migration of the allelic sequences on the sequencing gel. Cycling conditions were 50 cycles of 95ºC for 30 s, 50ºC for 30 s, and 60ºC for 7 minutes.

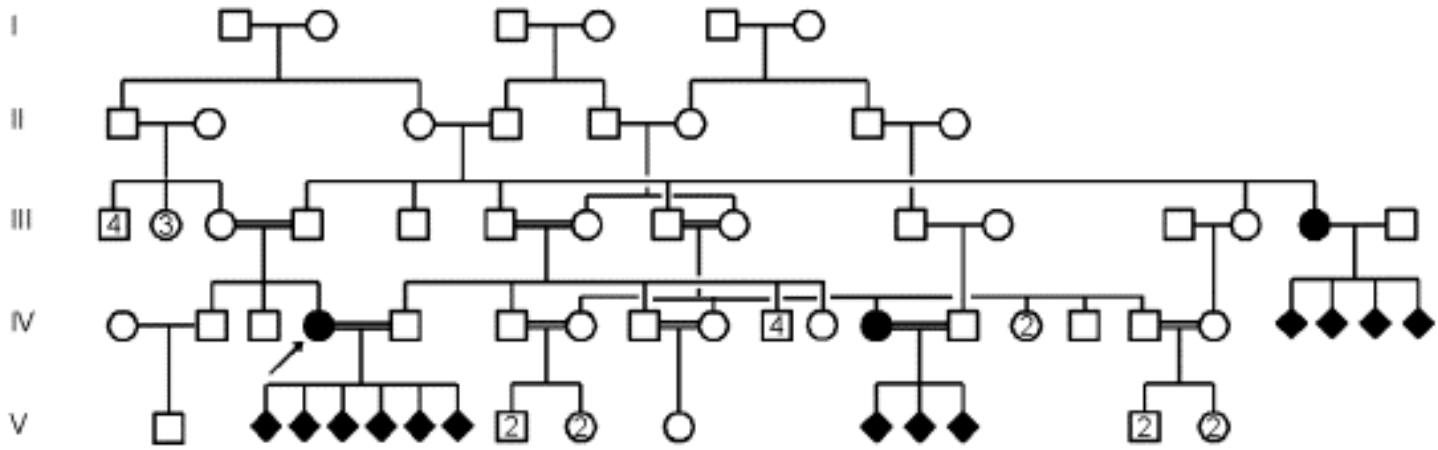

Figure 1. Pedigree of BiCHM family.

Filled diamonds indicate molar pregnancies. The index case IV:4 is arrowed. Known consanguineous matings are indicated by double bars. Filled circles indicate affected women (presumed homozygous by descent for the causative mutation), who are, however, themselves phenotypically normal except during pregnancy. DNA from affected individuals IV:4 and III:14 was used for genetic analysis.

Marker	**Map position (Mb) www.ensembl.org**	**III:14**	**IV:4**
D19S418	67.5	84/84	84/86
D19S926	67.58	176/178	176/180
D19S605	67.9	113/117	115/117
CA025588	70.6		181/193
D19S887	70.7	245/253	253/253
GT011499 = D19S404	70.7		100/110
D19S573	70.3	225/225	225/229
D19S210	70.1	165/175	165/175
D19S214	70.9	164/170	170/178
D19S218	71.3	203/217	203/217
DNMT3L	**42.4**		
D21S1411	41.0	287/291	287/291
D21S1912	42.4	213/239	213/239
D21S1446	44.8	208/208	208/224

Table 1. Genetic analysis of candidate BiCHM loci.

Homozygous markers are shaded in grey. Autozygosity mapping was previously used in two consanguineous families to suggest a BiCHM locus on 19q13.3-q13.4 (Moglabey et al. 1999, ref. 7 in main text). The genetic map in this candidate region was reported as: D19S418-2.1-(D19S926/

D19S605)-5.2-D19S887-0.1-(D19S573/D19S210)-1.2-D19S214-1.3-D19S218 (with distances in centiMorgans). None of the markers within this previously suggested linkage interval is homozygous in both affected women available in the present family. Because of the 5 cM gap between D19S605 and D19S887, respectively heterozygous and homozygous in IV:4, we additionally identified and typed two markers that flank D19S887 by <100 kb on each side. Both these markers (CA025588 and GT011499, identical to D19S404) being heterozygous in IV:4, homozygosity by descent for D19S887 was ruled out. Recessive mutation of the mouse *Dnmt3L* gene prevents maternal imprint establishment and causes male sterility. This gene does not appear to be involved in our BiCHM family since there is no homozygosity by descent for markers closely surrounding it (marker order D21S1411-*DNMT3L*-D21S1912).

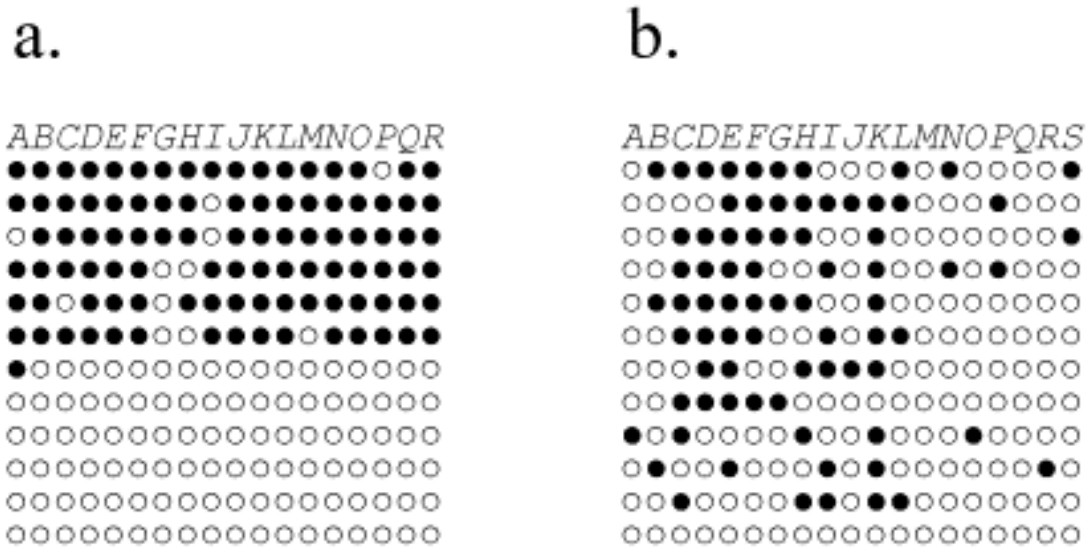

Figure 2. Clonal analysis of bisulphite-PCR products from BiCHM.

Methylation analysis was mostly performed as described above by direct sequencing of bisulphite-PCR products, since this avoids problems of cloning bias at some loci. However, some loci displaying a mixed methylation pattern on direct sequencing were analysed by cloning to assess the allele-specificity of this methylation. One clone per horizontal line; black symbol = methylated residue; white symbol, unmethylated residue. **a,** *H19***.** Labelling of CpGs is as in Kerjean et al., ref. 11 in main text. The distribution of methylated and unmethylated CpGs is indistinguishable from that in normal somatic tissues. It is consistent with unimpaired establishment and maintenance of a paternal imprint at *H19* in the BiCHM. **b,** *GNAS1-XLαs.* This, as discussed in the main text, was the only maternally methylated DMR not to show clear evidence of a defect in the BiCHM on direct sequencing. This retention of differential methylation has also been noted in some PHP-Ib patients with *cis*-acting imprinting mutations at this locus. However, the cloned BiCHM *GNAS1-XL* products show a strikingly different appearance from that of *H19*. This suggests that the appearance on direct sequencing does not reflect normal imprinting at *GNAS1-XL*, but a rather disordered scattering of methylated residues across both alleles.

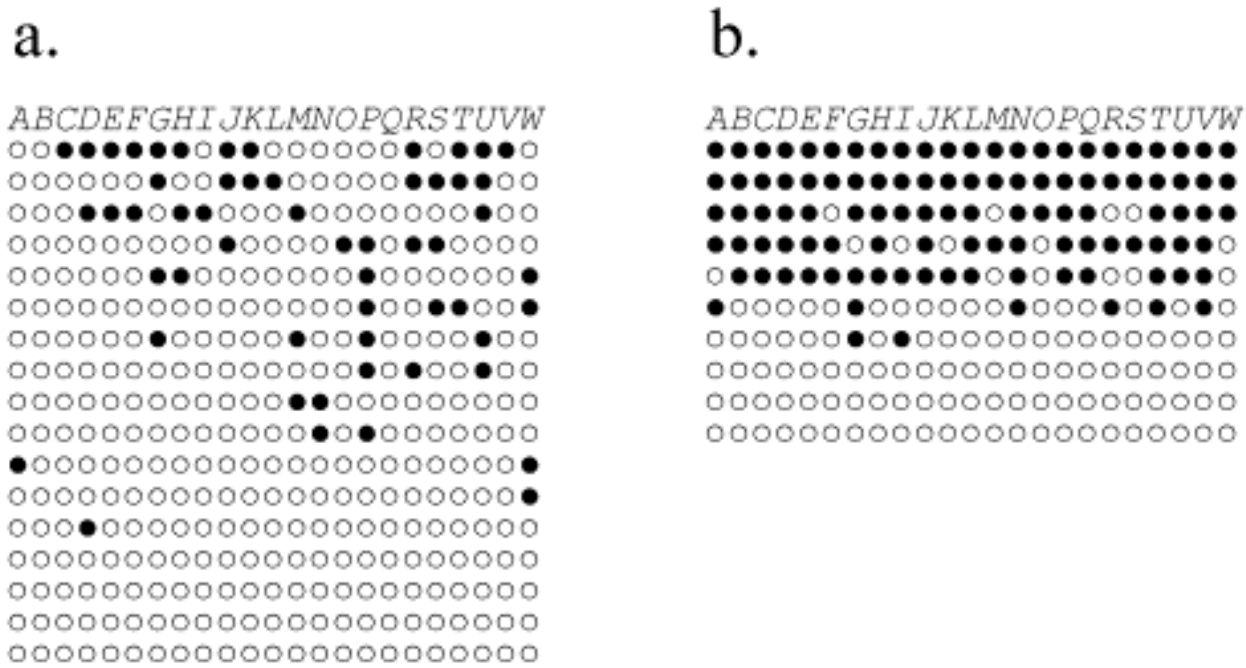

Figure 3. Clonal analysis of bisulphite-PCR products from AgCHM.

At several loci, the BiCHM methylation pattern is indistinguishable from that of AgCHM (*H19* representing an important predicted exception). However, at four DMRs (*PEG1*, *KCNQ1OT1*, *SNRPN* and *GNAS1*-1A), the BiCHM epigenotype actually appears even more purely "paternal" than that of the AgCHM. The reason for this is unclear, though it implies that the presence of an extra paternal allele (rather than an abnormal maternal one) increases the susceptibility of the CHM to acquiring abnormal postzygotic methylation changes. The failure of AgCHM to conform perfectly to the expected paternal methylation pattern has been reported previously[2]. There is also evidence that early uniparental mouse embryos may "adjust" methylation patterns towards those of normal biparental embryos, perhaps implying the existence of a dosage compensation

mechanism similar to that of X-inactivation[3]. Possibly, therefore, such a process could influence the methylation patterns eventually observed in the androgenetic moles. Two examples of clonal analysis of AgCHM are shown.**a**, *SNRPN.* Figure 1c in the main text shows that both AgCHM displayed a minor degree of *SNRPN* DMR methylation (normally only seen on a maternal allele). The clones show a striking contrast to the strictly haplomethylated pattern we show above for *H19* in the BiCHM. Our interpretation is that a degree of secondary methylation is occurring in AgCHM, but that it is incomplete and quite probably not allele-specific. The overall proportion of methylated C residues (14%) agrees with visual assessment of the directly sequenced PCR product. **b**, *GNAS1-1A.* Figure 2 in the main text indicates that one of the AgCHM showed approximately equal intensity of methylated and unmethylated signals at all the CpG positions. *GNAS1-1A* clones from this AgCHM are either almost completely methylated or unmethylated. It is unclear whether or not this reflects allele-specificity, since we cannot distinguish the two paternal alleles at this locus. It remains possible that the pattern results not from allele-specificity, but from cooperative kinetics of *de novo* methylation.

References

1. Zeschnigk, M. *et al.* Imprinted segments in the human genome: different DNA methylation patterns in the Prader-Willi/Angelman syndrome region as determined by the genomic sequencing method. *Hum Mol Genet* **6**, 387-95 (1997).

2. Arima, T., Matsuda, T., Takagi, N. & Wake, N. Association of IGF2 and H19 imprinting with choriocarcinoma development. Cancer Genet Cytogenet 93, 39-47 (1997).

3. Shemer, R. *et al.* Dynamic methylation adjustment and counting as part of imprinting mechanisms. *Proc Natl Acad Sci U S A* **93**, 6371-6 (1996).